Histol Histopathol (2025) 40: 935-946

Histology and Histopathology
From Cell Biology to Tissue Engineering

ORIGINAL ARTICLE Open Access

E2F1-induced upregulation of *TROAP* contributes to endometrial cancer progression

Shanshan Wang[1]*, Yidan Sun[1]*, Minjing Guo[1]*, Ping Zhu[2] and Beibei Xin[1]

[1]Department of Gynecology and Obstetrics and [2]Department of Reproductive Medicine, Yantai Yuhuangding Hospital, Yantai, Shandong, China

*These authors contributed equally to this work

Summary. Purpose. To investigate the role of Trophinin-associated protein (TROAP) in endometrial cancer (EC) progression and elucidate how the transcription factor E2F transcription factor 1 (E2F1) modulates EC by upregulating *TROAP* expression.

Methods. *TROAP* expression in EC tissues and cell lines was analyzed using bioinformatics databases, quantitative real-time polymerase chain reaction (qRT-PCR), western blot, and immunohistochemistry. *TROAP* was knocked down in EC cells to assess its effects on proliferation, migration, invasion, and glycolysis. Potential transcription factors regulating *TROAP* were identified, and the relationship between E2F1 and *TROAP* gene regulation was examined using dual luciferase assay. *In vivo* tumor growth was evaluated using a mouse xenograft model.

Results. *TROAP* was overexpressed in EC tissues and cell lines compared with normal controls. High *TROAP* expression correlated with poor differentiation, advanced stage, lymph node metastasis, and worse overall survival in EC patients. Knockdown of *TROAP* inhibited the proliferation, migration, invasion, and glycolytic capacity of EC cells. E2F1 was identified as a transcriptional activator of TROAP. E2F1 overexpression enhanced *TROAP* expression and promoted EC cell proliferation, migration, and glycolysis in a *TROAP*-dependent manner. *TROAP* knockdown suppressed tumor growth *in vivo*.

Conclusion. TROAP is transcriptionally activated by E2F1 and promotes EC progression by enhancing cell proliferation, metastasis, and glycolysis. The E2F1-TROAP axis may serve as a potential therapeutic target for EC treatment.

Corresponding Author: Ping Zhu, No. 20 East Yuhuangding Road, Yantai 264000, China. e-mail: zhuzp111@126.com or Beibei Xin, No. 20 East Yuhuangding Road, Yantai 264000, China. e-mail: Xbeibei93@163.com

www.hh.um.es. DOI: 10.14670/HH-18-834

Key words: Endometrial cancer, Transcription factor, E2F1, TROAP, Pathogenesis

Introduction

Endometrial cancer (EC) is a heterogeneous malignancy of the female reproductive system (Watanabe et al., 2021). In 2019, approximately 65,950 new EC cases and 12,550 EC-related deaths were reported in the United States, with a projected global increase in EC incidence by 2025 (Callender et al., 2019; Siegel et al., 2022). Early EC symptoms are subtle, however, advanced disease may present with abnormal uterine bleeding, leukorrhea, and pelvic pain (Urick and Bell, 2019). Current treatments include surgery, chemotherapy, and radiotherapy (Brooks et al., 2019). Despite favorable survival rates for early-stage EC, limited therapeutic options and high metastatic and recurrent potential lead to poor overall survival and prognosis in advanced cases (Walsh et al., 2023). Recent genetic studies have provided new insights into EC pathogenesis and treatment (Retis-Resendiz et al., 2021; Watanabe et al., 2021; Xu et al., 2022).

TROAP (Trophinin-associated protein), initially characterized in embryonic trophoblast cells, is crucial for early embryo implantation, rapid cell invasion, and proliferation (Lian et al., 2018). TROAP regulates spindle formation during mitosis, with overexpression causing unipolar spindles and decreased expression leading to mitotic arrest and multipolar spindles (Zhao et al., 2021). The *TROAP* gene was first characterized in 1995 by Fukuda et al. during their investigation of trophoblast-endometrial cell adhesion. They discovered that co-expression of *TROAP* and *TRO* genes conferred adhesion ability to previously non-adhesive COS cells (Fukuda and Sugihara, 2012a). *TROAP* and *TRO* expression peaks during embryo implantation, suggesting roles in embryonic cell proliferation and trophoblast invasion (Fukuda et al.,1995). In normal tissues, *TROAP* is highly expressed in the testis, bone

marrow, small intestine, thymus, and fetal liver but is low or absent in most other tissues (Fukuda and Sugihara, 2012b). Recent studies have reported high TROAP expression in human cancer cell lines (Jiao et al., 2019; Li et al., 2019). In hepatocellular carcinoma, *TROAP* overexpression is associated with shorter median overall survival and may serve as an independent prognostic predictor (Jiao et al., 2019). Additionally, TROAP enhances breast cancer cell proliferation, invasion, and metastasis (Li et al., 2019). However, its potential role in EC progression remains to be explored.

In the present study, we analyzed *TROAP* expression in EC and its relationship with patient prognosis. Using two representative EC cell lines, we also examined the effects of *TROAP* knockdown on cell proliferation, metastasis, and glycolysis. Additionally, we identified E2F1 (E2F transcription factor 1), which has been implicated in tumor progression (He et al., 2018; Zhao et al., 2019; Iglesias et al., 2020), as a potential upstream regulator of *TROAP* gene expression using bioinformatic databases. Therefore, we further determined the regulatory relationship between E2F1 and *TROAP* expression in EC. These findings not only enhance our understanding of the molecular mechanisms underlying EC progression but also highlight the potential of the E2F1-TROAP axis as a promising therapeutic target for EC treatment.

Materials and methods

Bioinformatics analysis

Patient data for 581 EC cases were obtained from The Cancer Genome Atlas (TCGA) database to examine the correlation between the *TROAP* gene and prognosis of EC patients. The University of Alabama at Birmingham Cancer Data Analysis Portal (UALCAN) website (http://ualcan.path.uab.edu/analysis-prot.html) was used to analyze *TROAP* expression in EC. The UALCAN database was also used to analyze the expression of E2F1 mRNA. The PROMO (Prediction of Transcription Factor Binding Sites) database (https://alggen.lsi.upc.es/cgi-bin/promo_v3/promo/promoinit.cgi?dirDB=TF_8.3) was used to identify potential transcription factors for the *TROAP* gene, and the JASPAR (Journal of Algorithms for Structural and Physical Analysis of Regulatory Sequences) website (http://jaspar.genereg.net/), a database of transcription factor binding profiles, was used to analyze potential binding sites of TROAP promoter sequences to transcription factor E2F1. The Kaplan-Meier Plotter website (http://kmplot.com/analysis/index.php?p=back-ground), a tool for meta-analysis-based biomarker assessment, was used to analyze the relationship between *TROAP* expression levels and EC prognosis, and the correlation between E2F1 and *TROAP* expression was analyzed through the UALCAN database.

Tissue collection

To investigate the potential correlation between *TROAP* expression levels and EC patient prognosis, 48 pairs of EC tissues and corresponding adjacent tissues were collected from EC patients who underwent surgery at our hospital between January 2019 and December 2022. The patients were all females, aged 40-74 years (mean age: 52.6 years). The study procedures involving the usage of human tissues were approved by the Medical Ethics Committee of Yantai Yuhuangding Hospital and performed in compliance with institutional ethical standards. Informed consent for clinical research was obtained from all patients.

Cell culture

The EC cell lines RL95-2, HEC-1A, HEC-1B, and Ishikawa, and the human immortalized endometrial stromal cell line HESCs (CellBank, Shanghai, China) were cultured in RPMI 1640 medium containing 10% FBS, 100 U/mL penicillin, and 100 μg/mL streptomycin (GIBCO, CA, USA) in a 37°C, 5% CO_2 incubator with saturated humidity. The cells were maintained until reaching the logarithmic growth phase, as confirmed by microscopic observation.

Cell transfection

TROAP knockdown, E2F1 overexpression lentiviral vector, and negative control were obtained from Ribobio (Guangzhou, China). All cell lines were maintained consistently in RPMI 1640 medium supplemented with 10% fetal bovine serum. EC cells were seeded in six-well plates and, once they reached 85% confluence, shRNA-TROAP, shRNA-NC, vector, and E2F1 were transiently transfected using the Lipofectamine 2000 kit (Thermo Fisher Scientific, CA, USA). For stable *TROAP* knockdown in EC cells, lentiviral constructs were employed. EC cells at the logarithmic growth phase were plated in six-well plates at a density of 5×10^4 cells per well and incubated at 37°C for 24 hours. Lentivirus was added at a multiply of infection (MOI) of 10 for 48 hours. Infection efficiency was evaluated using fluorescence microscopy 72 hours post-infection. Post 72 hours, the medium was refreshed with complete medium containing 2 μg/mL puromycin (Sigma, St. Louis, MO, USA) for a one-week selection. The puromycin concentration was subsequently reduced to 1 μg/mL for another two weeks to generate cell clones stabling expressing the shRNA construct.

qRT-PCR

RNA samples were extracted from tissue or cultured cells utilizing a total RNA extraction kit (Omega BioTek, Vermont, USA) and examined with a UV spectrophotometer to assess the purity of the total RNA. A total of 500 ng of the extracted RNA underwent

reverse transcription into cDNA via a reverse transcription kit (QIAGEN, Hilden, Germany). Subsequently, cDNA samples were diluted 20 times and served as the template for quantitative PCR analysis using the Premix Ex Taq quantitative PCR kit (Roche Inc., Basel, Switzerland). The conditions for the PCR reaction were established as follows: an initial denaturation step at 95°C for 10 minutes, followed by annealing at 95°C for 15 seconds, extension at 58°C for 30 seconds, and a final extension phase at 72°C lasting 30 seconds, for a total of 35 cycles. The analysis of the results was conducted using the $2^{-\Delta\Delta Ct}$ method.

The forward sequence for *TROAP* was 5'-CCTCC GGGGTGTGTATCTCCTAC-3', and the reverse sequence was 5'-ACGGCGCACGATGTAACAG-3'; the forward sequence for *E2F1* was 5'-ACGGCGCACG ATGTAACAG-3', and the reverse sequence was 5'-ACGGCGCGCACGATGTAACAG-3'; the forward sequence for *GAPDH* was 5'-CGACCACTTTGTC AAGCTCA-3', and the reverse sequence was 5'-GGTTGAGCACAGGGTACTTTATT-3'. *GAPDH* was used as an internal reference gene.

Western blot analysis

The collection of protein samples was performed using RIPA buffer to extract total proteins, which were then quantified with the BCA method. The protein concentration was measured utilizing the BCA protein assay kit obtained from Beyotime (Beijing, China). From each experimental condition, 30 μg of protein was used for polyacrylamide gel electrophoresis. Separated target proteins and protein ladders were transferred onto a polyvinylidene difluoride (PVDF) membrane. This membrane was blocked using 5% skimmed milk powder at room temperature for 1 hour. The membranes were then incubated with primary antibodies [Anti-TROAP (catalog: sc-373714, Santa Cruz, 1:500), Anti-E2F1 (catalog: sc-251, Santa Cruz, 1:500), Anti-GAPDH (catalog: sc-365062, Santa Cruz, 1:4000)], followed by incubation with an HRP-linked secondary antibody (ab7090, 1:2000). Image acquisition was performed using ECL Plus (Life Technologies, USA) chemiluminescence systems and the bands were quantified using ImageJ software. The relative expression levels of the target proteins in each group were calculated by comparing grayscale values, with GAPDH serving as the internal control.

CCK-8 assay

Cell proliferation was evaluated with a CCK-8 kit (CCK-8, Dojindo, Japan). A total of 5×10^3 EC cells per well were plated in 96-well plates 48 hours after transfection. At 24-hour intervals, the plates were examined using a microscope, and CCK-8 solution was applied and allowed to incubate for 2 hours. The optical density (OD) readings were captured using an enzyme marker at 450 nm, and outcomes were consistently monitored for 96 hours and documented.

EdU staining

The number of actively dividing cells was quantified following the protocols provided in the EdU staining kit (C00788L, Beyotime, China). An EdU solution at a working concentration of 50 μmol/L was prepared using complete medium and cells were incubated with EdU-containing medium for 2 hours. Subsequently, the medium was removed, and cells were rinsed twice with PBS. The samples were then fixed with 4% paraformaldehyde and stained using an Apollo reaction mixture for 1 hour at room temperature. After the counter-staining of nuclei, the detection of EdU-incorporating cells was carried out under a fluorescence microscope.

Transwell experiments

Transwell experiments were conducted to assess cell migration and invasion. For each assay, 2×10^4 cells in 200 μL serum-free medium were seeded in the upper chamber of a Transwell insert (8 μm pore size, Corning) with a non-coated membrane (for migration assays) or a Matrigel-coated membrane (1:8 dilution, BD Biosciences, for invasion assays). The lower chamber was filled with 600 μL of medium containing 10% FBS as a chemoattractant. Cells were incubated for 24 hours (migration) or 48 hours (invasion) at 37°C in 5% CO_2. After incubation, cells that did not migrate or invade through the pores were carefully removed with a cotton swab. Cells on the lower surface of the membrane were fixed with 4% paraformaldehyde for 15 minutes and stained with 0.1% crystal violet solution for 30 minutes at room temperature. After gentle washing with PBS, the membranes were air-dried. Stained cells were visualized under a light microscope (Olympus BX51) at 200× magnification. Five random fields per membrane were photographed using a digital camera attached to the microscope. The number of migrated or invaded cells was counted using ImageJ software (NIH), and the average number of cells per field was calculated.

Dual-luciferase reporter assay

Cells were cultured and transfected as described in section 2.3. The *TROAP* promoter region (-2000 to +100 bp relative to the transcription start site) was amplified by PCR from the genomic DNA of HEC-1A cells. The wild-type (WT) or mutant (MUT) *TROAP* promoter sequences were cloned and integrated into the pGL3-Basic vector (Promega, MA, USA) using KpnI and XhoI restriction sites to construct pGL3-*TROAP* WT and pGL3-*TROAP* MUT luciferase reporter gene plasmids. The mutant construct contained specific mutations in the predicted E2F1 binding sites. HEC-1A and Ishikawa cells were seeded in 24-well plates at a density of 5×10^4 cells per well. After 24 hours, cells were co-transfected

with 500 ng of pGL3-*TROAP* WT or pGL3-*TROAP* MUT plasmids, along with 50 ng of pRL-TK Renilla luciferase plasmid (Promega) as an internal control, using Lipofectamine 3000 (Invitrogen) according to the manufacturer's protocol. After 48h of transfection, cells were lysed with 100 μL of Passive Lysis Buffer (Promega) at room temperature for 20 min, the supernatant was collected by centrifugation at 12,000 g for 5 minutes, and 20 μL of the lysate was transferred to a white 96-well plate. The luciferase substrate was added to measure enzyme activity using the Dual-Luciferase Reporter Gene Assay Kit (Promega). Luminescence was measured using a GloMax 20/20 luminometer (Promega). The relative activity of firefly luciferase was calculated using Renilla luciferase activity as an internal reference.

Metabolic assays

EC cells (2×10^5 cells/well) were seeded in 12-well plates for 24 hours. For the glucose consumption assay, the medium was replaced with 5 mM glucose-containing medium. After 24 hours, 50 μL of medium was collected and glucose utilization was quantified using a glucose assay kit (Megazyme International Ireland Ltd., Wicklow, Ireland). Absorbance was measured at 505 nm. For the lactate level assay, 50 μL of culture medium was collected after 24 hours and lactate concentrations were determined using a lactate assay kit (Megazyme International Ireland Ltd.). Absorbance was measured at 530 nm. For ATP quantification, cells were lysed with ATP assay buffer. ATP concentrations were measured using an ATP assay kit (Merck Millipore, Burlington, MA, USA). Luminescence was measured at 562 nm. All assays were performed in triplicate using a microplate reader (BIO-RAD Laboratories, Hercules, CA, USA). Results were normalized to protein concentration and expressed as the mean ± standard deviation of three independent experiments.

Immunohistochemistry

Immunohistochemistry was performed to detect TROAP and Ki-67 expression in EC tissues. Formalin-fixed, paraffin-embedded tissue sections (4 μm) were deparaffinized, rehydrated, and subjected to antigen retrieval. Sections were incubated with primary antibodies [Anti-Ki67 (MA5-14520, Invitrogen, 1:200) and Anti-TROAP (PA5-60613, Invitrogen, 1:100)] overnight at 4°C, followed by an HRP-conjugated secondary antibody (A11001, Invitrogen, 1:500) for 1 hour. Visualization was achieved using a DAB Substrate Kit (Vector Laboratories) and hematoxylin counter-staining. Images were captured using an Olympus BX53 microscope. TROAP and Ki-67 expression were evaluated based on positive cell percentage. Five randomly selected high-magnification fields of view were scored for the percentage of positivity. All sections were analyzed by two pathologists.

Construction of a subcutaneous xenograft mouse model

The animal studies were approved by the Animal Ethics Committee of Yantai Yuhuangding Hospital. A total of twenty five-week-old BALB/c nude mice were obtained from Beijing Viton Lihua Laboratory Animal Technology Co., Ltd. (Beijing, China). The mice were randomly divided into two groups (n=10 in each group): the sh-NC and sh-TROAP groups, each inoculated with the corresponding HEC1A cells. Cells with viability exceeding 98% were harvested and subcutaneously injected near the axilla at a density of 5×10^6 cells in 100 μL per site. Tumor growth was monitored by measuring the long (L) and short (W) diameters every 7 days using calipers, and volume was calculated as $L\times W^{2/2}$. After 35 days, the mice were humanely euthanized, and tumors were excised, weighed, and processed for immuno-histochemical analysis of Ki-67 and TROAP expression, as well as protein blotting.

Statistical snalysis

Experiments were performed in triplicate. Data were analyzed using SPSS software (Version 28.0, IBM Corp) and presented as mean ± standard deviation. Comparisons between groups were made using independent t-tests (two groups) or one-way ANOVA (multiple groups). Correlations between clinical characteristics and protein expression were analyzed using χ^2 tests. Kaplan-Meier curves were used to analyze the correlation between *TROAP* mRNA expression and overall survival in EC patients. Statistical significance was set at $p<0.05$.

Results

TROAP overexpression in EC tissues and cells

To investigate *TROAP* expression in endometrial cancer (EC), we analyzed data from TCGA using the UALCAN database. *TROAP* mRNA expression levels were significantly elevated in EC tissues compared with normal tissues (Fig. 1A). We validated these findings using qRT-PCR in 48 EC patient samples, confirming *TROAP* upregulation in tumor tissues relative to adjacent normal tissues (Fig. 1B). Immunohistochemical staining and western blot analysis further corroborated these results, showing an upregulated level of TROAP protein in EC tissues (Fig. 1C,D).

Furthermore, Chi-square analysis revealed significant associations between high *TROAP* expression and poor differentiation, advanced FIGO stage, and positive lymph node metastasis in EC tissues (Table 1). However, *TROAP* expression showed no significant differences among various subtypes, indicating that it is not affected by subtypes. Kaplan-Meier survival analysis of TCGA data demonstrated that patients with high *TROAP* expression had significantly lower overall survival compared with those with low expression

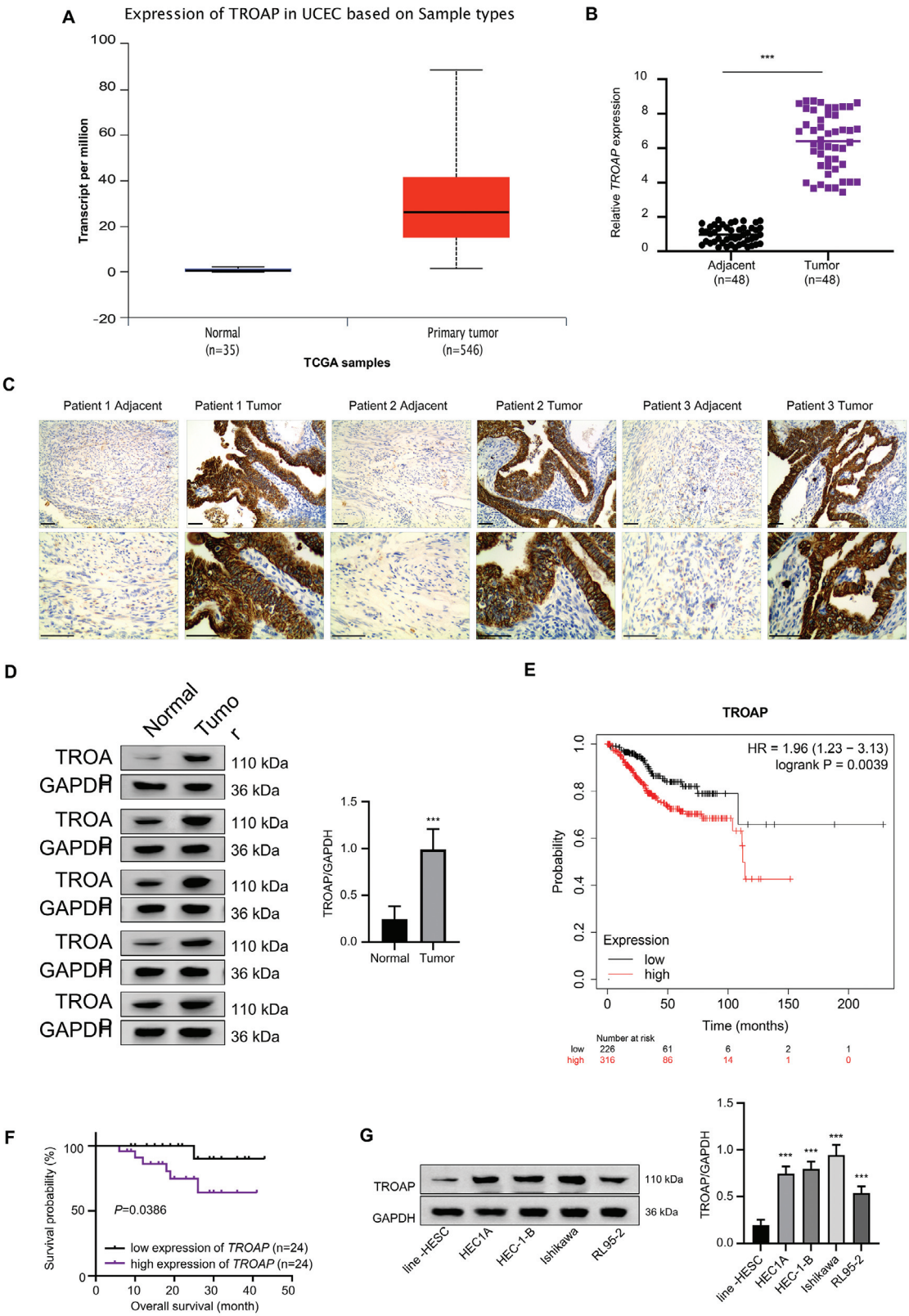

Fig. 1. *TROAP* is highly expressed in endometrial cancer tissues and cells. **A.** UALCAN analysis of TCGA-EC data revealed that *TROAP* was significantly overexpressed in endometrial cancer compared with normal tissue. **B.** qRT-PCR analysis of *TROAP* expression in 48 paired EC tumors and adjacent normal tissue showed significantly higher levels in tumor samples. **C.** Immunohistochemical staining of three paired EC and normal tissue samples demonstrated markedly increased TROAP protein levels in tumors. Scale bars, 50 μm. **D.** Western blot analysis demonstrated markedly increased TROAP protein levels in EC tumor tissues. **E.** Kaplan-Meier Plotter analysis revealed significantly poorer overall survival in EC cancer patients with high *TROAP* expression (p=0.0039). **F.** Kaplan-Meier survival analysis of 48 EC patients stratified by *TROAP* expression showed significantly shorter overall survival in the high expression group (n=24) compared with the low expression group (n=24) (p=0.0386). **G.** Western blot analysis of TROAP protein levels in EC cell lines (HEC1A, HEC1B, Ishikawa, and RL95-2) and normal endometrial HESCs demonstrated substantially higher expression in cancer cells. **p<0.01, ***p<0.001 compared with normal HESCs or the paraneoplastic tissue group.

(p=0.0039; Fig. 1E). This finding was independently confirmed in our cohort of 48 EC patients, where the high *TROAP* expression group (n=24) showed significantly poorer survival than the low expression group (n=24) (p=0.0386; Fig. 1F). At the cellular level, we also observed significantly elevated TROAP protein expression in EC cell lines (HEC1A, HEC1B, Ishikawa, and RL95-2) compared with the normal endometrial cell line HESCs (Fig. 1G). Collectively, these findings suggest a potential oncogenic role for TROAP in EC pathogenesis and progression.

TROAP knockdown suppresses EC cell proliferation, mobility, and glycolysis

To elucidate the functional role of TROAP in EC cells, we conducted a series of *in vitro* assays after interfering with its expression. We initially applied the CRISPR/Cas9 technique to knock out the *TROAP* gene in EC cells. However, we failed to generate stable knockout cell clones since cells underwent spontaneous cell death once the *TROAP* gene was knocked out. Instead, we applied shRNA-mediated gene silencing to conduct loss-of-function experiments. Western blot analysis demonstrated a significant reduction in TROAP expression in the shRNA-TROAP-1/2/3 groups compared with the shRNA-NC group. The most effective construct, shRNA-TROAP-1, was selected for subsequent experiments (Fig. 2A). Having established effective TROAP knockdown, we proceeded to investigate its functional consequences. First, CCK-8 assays revealed significantly reduced cell growth capacity in the shRNA-TROAP group compared with the shRNA-NC group (Fig. 2B). To further confirm this effect on cell growth, EdU assays were performed, showing that the number of EC cells undergoing DNA synthesis was significantly suppressed following *TROAP* knockdown (Fig. 2C). Next, we examined the impact of *TROAP* silencing on cell motility. Transwell assays demonstrated that both cell migration and invasion capabilities were significantly impaired after TROAP interference (Fig. 2D,E). Finally, we investigated whether TROAP affects cellular metabolism. Metabolic assays revealed that the sh-TROAP group exhibited significantly decreased glucose consumption, as well as lower levels of lactate production and intracellular ATP generation (Fig. 2F). Taken together, these findings collectively indicate that *TROAP* knockdown inhibits cell proliferation, invasion, and glycolytic activity in EC cell lines, suggesting a multifaceted role for TROAP in promoting EC progression.

E2F1 serves as a potential transcription activator for TROAP

To investigate the regulatory mechanisms governing *TROAP* expression in EC, we sought to identify potential upstream transcription factors. We utilized two databases (JASPAR and PROMO) to predict potential upstream transcription factors of *TROAP* and cross-referenced these with UALCAN online analysis of genes positively associated with *TROAP* expression in TCGA-EC data. This comprehensive approach identified 164 potential upstream transcription factors of *TROAP* and 1053 genes positively associated with *TROAP* expression. A Venn analysis of these genes revealed E2F1 as a potential upstream transcription factor of *TROAP* (Fig. 3A). To validate this prediction, we constructed cell models with E2F1 expression interference or E2F1 overexpression (Fig. 3B). TROAP protein expression was reduced after E2F1 knockdown, while E2F1 overexpression increased its expression level (Fig. 3C). To further confirm the regulatory relationship, we analyzed the *TROAP* promoter region for E2F1 binding sites using the JASPAR website, revealing consensus binding sequences (Fig. 3D). Building on this finding, we performed a dual luciferase reporter gene assay, which showed that the activity of the WT *TROAP* promoter significantly increased when exogenous E2F1 was introduced, whereas the activity of the MUT *TROAP* promoter did not significantly change (Fig. 3E). These findings collectively indicate the regulation of the *TROAP* gene by E2F1.

To corroborate these *in vitro* findings with clinical

Table 1. Association between *TROAP* expression and clinicopathological features of patients with endometrial cancer.

Clinical characters	*TROAP* expression		*p* value
	High (>median)	Low (≤median)	
Age(years)			
≤55	15	12	0.383
>55	9	12	
Menopause			
No	14	11	0.386
Yes	10	13	
Tumor size			
≤30 mm	8	11	0.146
>30 mm	16	13	
Histological differentiation			
Poor	9	2	0.046*
Well	15	22	
FIGO Stage			
I +II	12	20	0.014*
III +IV	12	4	
Lymph node metastasis			
N0	16	22	0.033*
N1	8	2	
Histological type			
Endometroid adenocarcinoma	17	21	0.404
Serous papillary adenocarcinoma	5	3	
Clear cell adenocarcinoma	1	0	
Squamous cell carcinoma	1	0	

Correlation between the clinicopathological characteristics of EC patients and *TROAP* expression levels. Using the median *TROAP* expression value of EC tissues in Fig.1B as the cut-off value, 48 EC patients were divided into the *TROAP* low-expression (n=24) and *TROAP* high-expression groups (n=24), and the Chi-square test was utilized to statistically correlate *TROAP* expression with clinicopathological data.

data, we analyzed EC data in the TCGA database, which suggested a significant positive correlation between E2F1 and *TROAP* expression (Fig. 3F). Consistent with this, qRT-PCR results from our collected clinical samples showed that the expression level of E2F1 in EC tissues was significantly higher than in normal tissues (Fig. 3G). Furthermore, correlation analysis revealed a positive association between E2F1 and *TROAP* at the mRNA level (r2=0.0322; Fig. 3H). Collectively, these results strongly suggest that E2F1 acts as an upstream

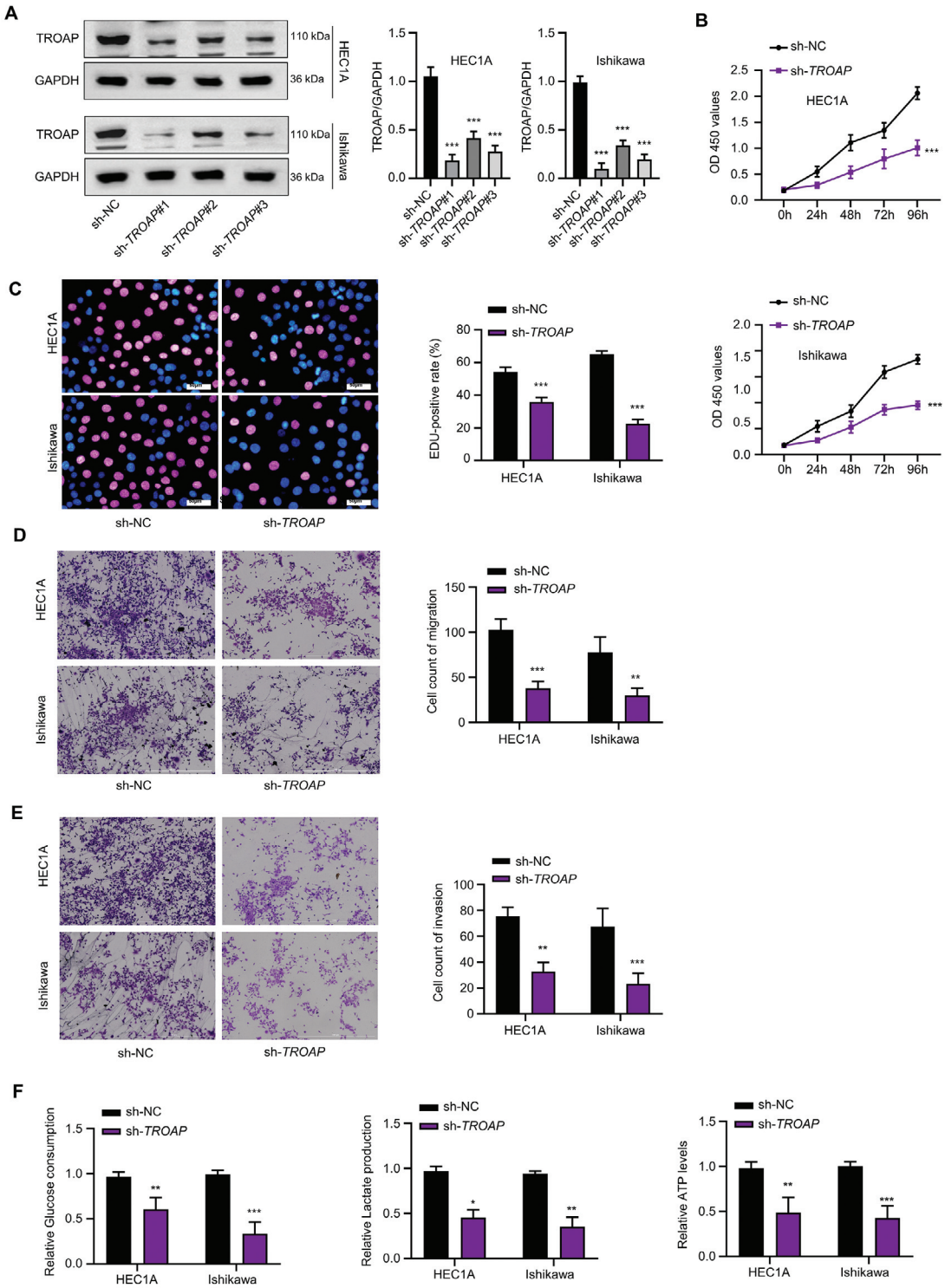

Fig. 2. Knockdown of TROAP inhibits EC cell proliferation, mobility, and glycolysis. **A.** Two EC cell lines (HEC1A and Ishikawa) with high TROAP expression were selected for knockdown. Western blot analysis confirmed efficient TROAP silencing in stable cell lines expressing lentiviral sh-TROAP#1, sh-TROAP#2, and sh-TROAP#3 compared with sh-NC controls. **B.** CCK-8 assay measuring absorbance at 450 nm at 0, 24, 48, 72, and 96 hours showed significantly reduced proliferation in *TROAP*-knockdown HEC1A and Ishikawa cells compared with sh-NC controls. **C.** The EdU assay revealed markedly decreased proliferation in *TROAP*-knockdown groups compared with sh-NC controls for both HEC1A and Ishikawa cells. Scale bars, 100 μm. **D.** Transwell migration assay (without Matrigel) demonstrated impaired migratory ability in *TROAP*-knockdown HEC1A and Ishikawa cells relative to sh-NC controls. Scale bars, 1000 μm. **E.** Transwell invasion assay (with Matrigel) showed reduced invasive capacity in *TROAP*-knockdown groups for both HEC1A and Ishikawa cells compared with sh-NC controls. Scale bars, 1000 μm. **F.** Measurement of glucose consumption, lactate production, and ATP levels revealed significant decreases in all three parameters in *TROAP*-knockdown HEC1A and Ishikawa cells *versus* sh-NC controls. *p<0.05, **p<0.01, ***p<0.001 compared with the sh-NC group.

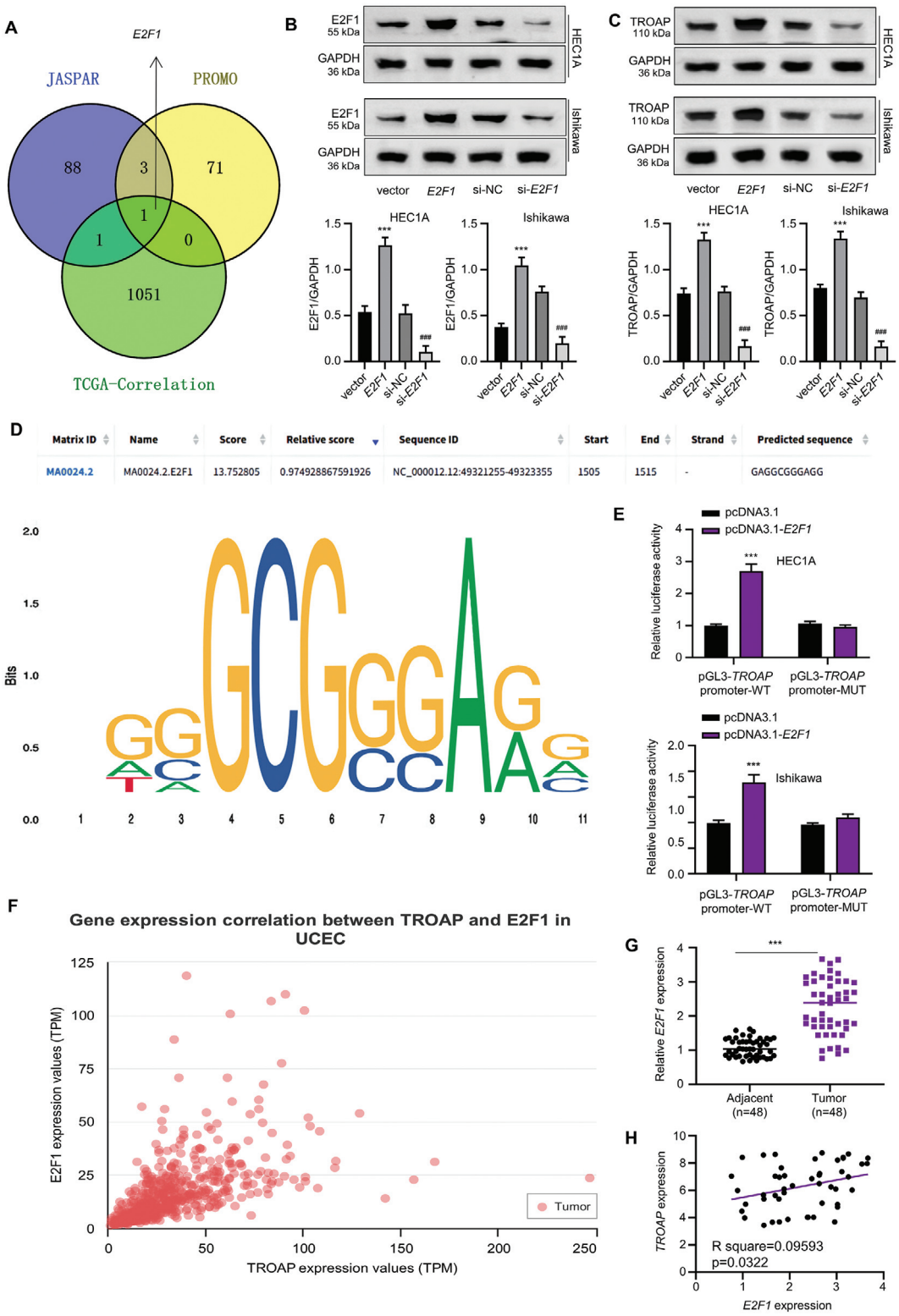

Fig. 3. E2F1 is a transcription factor regulating *TROAP* Expression. **A.** Integrative analysis of JASPAR and PROMO transcription factor predictions with UALCAN-derived *TROAP*-correlated genes in TCGA-EC data. **B.** Western blot analysis of E2F1 protein levels in HEC1A and Ishikawa cells with E2F1 overexpression or knockdown showed significant increases and decreases, respectively, compared to controls. **C.** Western blot analysis of TROAP protein levels in HEC1A and Ishikawa cells with E2F1 overexpression or knockdown demonstrated corresponding increases and decreases in TROAP expression. **D.** Schematic representation of JASPAR-predicted E2F1 binding sites and sequences in the *TROAP* promoter. **E.** Dual luciferase assay in HEC1A and Ishikawa cells co-transfected with E2F1 overexpression vector and wild-type or mutant *TROAP* promoter constructs. Significantly increased luciferase activity was observed with wild-type promoter and E2F1 overexpression, while the mutant promoter showed no response to E2F1. **F.** UALCAN analysis revealed a strong positive correlation between *TROAP* and E2F1 expression in the TCGA-EC dataset. **G.** qRT-PCR analysis of E2F1 expression in 48 paired EC tumors and adjacent normal tissues showed significantly higher levels in tumor samples. **H.** Correlation analysis demonstrated a significant positive association between E2F1 and *TROAP* expression in 48 EC tumor samples. $^{***}p<0.001$, $^{###}p<0.001$.

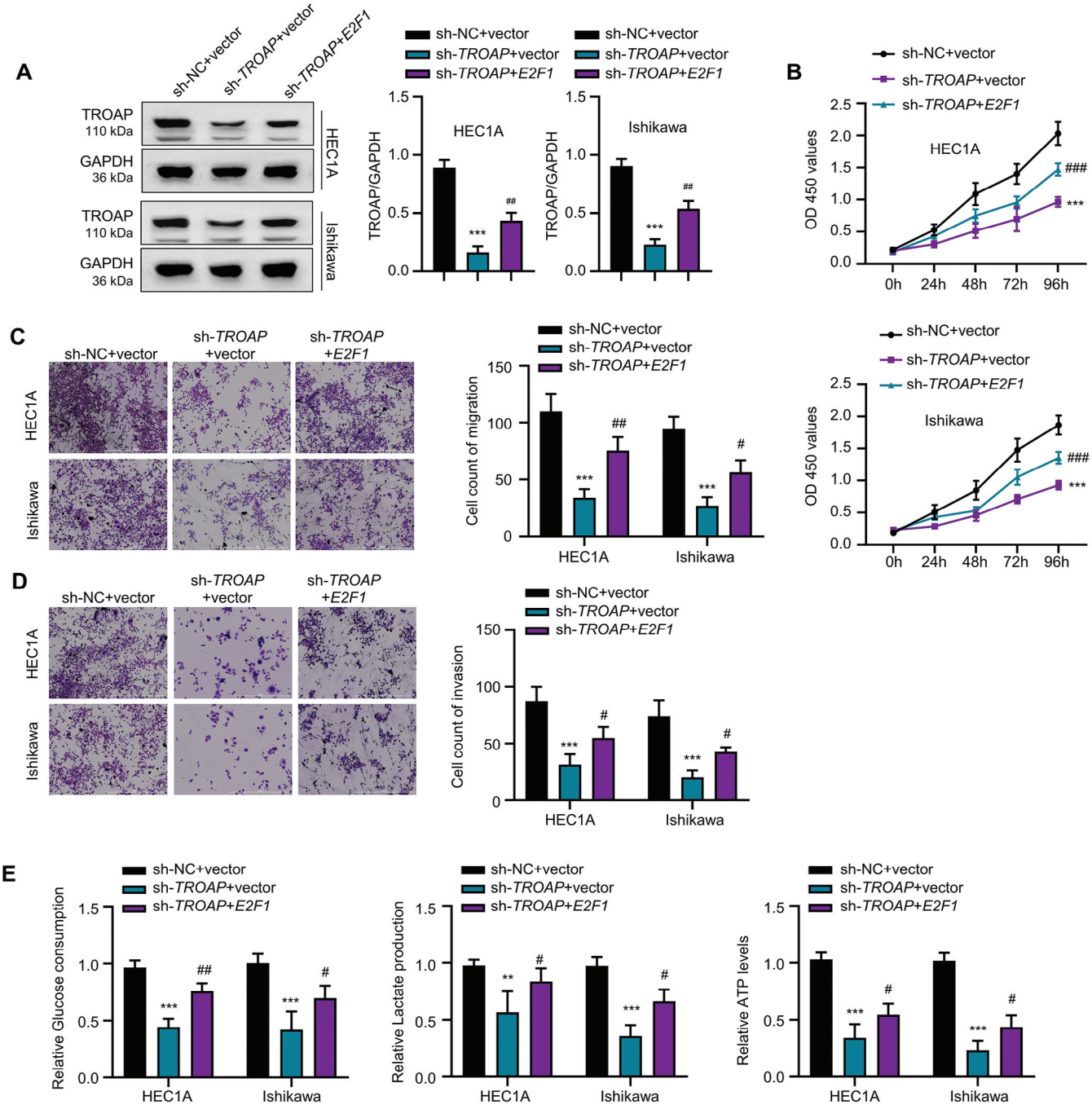

Fig. 4. Overexpression of E2F1 partially reverses the effects of *TROAP* knockdown on EC cells. **A.** Western blot analysis of TROAP protein levels in HEC1A and Ishikawa cells. *TROAP* knockdown significantly reduced expression, while E2F1 overexpression partially restored it. **B.** CCK-8 proliferation assay in HEC1A and Ishikawa cells. *TROAP* knockdown decreased proliferation, which was partially rescued by E2F1 overexpression. **C.** Transwell migration assay in HEC1A and Ishikawa cells. *TROAP* knockdown impaired migration, while E2F1 overexpression partially restored migratory capacity. Scale bars, 1000 μm. **D.** Transwell invasion assay in HEC1A and Ishikawa cells. *TROAP* knockdown reduced invasion, which was partially rescued by E2F1 overexpression. Scale bars, 1000 μm. **E.** Glycolysis parameters (glucose consumption, lactate production, and ATP levels) in HEC1A and Ishikawa cells. *TROAP* knockdown decreased all parameters, while E2F1 overexpression partially restored glycolytic activity. *p<0.01, ***p<0.001 vs sh-NC+vector; $^{\#}p$<0.05, $^{\#\#}p$<0.01, $^{\#\#\#}p$<0.001 vs. sh-TROAP+vector.

regulator of *TROAP* in EC, providing insight into the transcriptional control of this important oncogenic factor.

E2F1 overexpression partially reverses the effects of TROAP knockdown in EC cells

To elucidate the functional significance of the E2F1/TROAP axis in EC cells, we co-transfected E2F1 overexpression plasmids with shRNA-TROAP into HEC1A and Ishikawa cells. Notably, E2F1 overexpression partially restored TROAP protein levels following *TROAP* knockdown (Fig. 4A). We then comprehensively assessed the impact of this axis on EC cell behavior. CCK-8 assays revealed that *TROAP* knockdown significantly decreased EC cell proliferation, an effect partially reversed by E2F1 overexpression (Fig. 4B). Similarly, E2F1 overexpression partially rescued the impaired migratory and invasive capacity caused by *TROAP* silencing (Fig. 4C,D). Furthermore, measurements of glucose consumption, lactate production, and ATP levels showed that *TROAP* knockdown suppressed glycolysis, while E2F1 overexpression partially restored these metabolic parameters (Fig. 4E). Collectively, these findings strongly suggest that E2F1 promotes EC cell proliferation, invasion, and glycolysis primarily through *TROAP* activation, underscoring the critical role of the E2F1/TROAP axis in EC progression.

TROAP knockdown suppresses tumorigenesis of EC cells in vivo

To validate our *in vitro* findings and assess the role of *TROAP* in EC progression *in vivo*, we conducted xenograft experiments using HEC1A cells with *TROAP* knockdown. Subcutaneous xenograft experiments revealed significant differences between the sh-TROAP and sh-NC groups. Notably, tumors in the sh-TROAP group exhibited markedly reduced volume (Fig. 5A) and weight (Fig. 5B) compared with those in the sh-NC group. To further characterize the molecular changes in these tumors, we performed immunohistochemistry analyses. These studies demonstrated significantly decreased expression of both TROAP and Ki-67 (a well-established proliferation marker) in tumor tissues from the sh-TROAP group relative to the sh-NC group (Fig. 5C). Collectively, these *in vivo* results corroborate our *in vitro* findings, providing compelling evidence that *TROAP* knockdown effectively impedes the tumorigenic potential of EC cells.

Discussion

Endometrial cancer (EC) is the most common

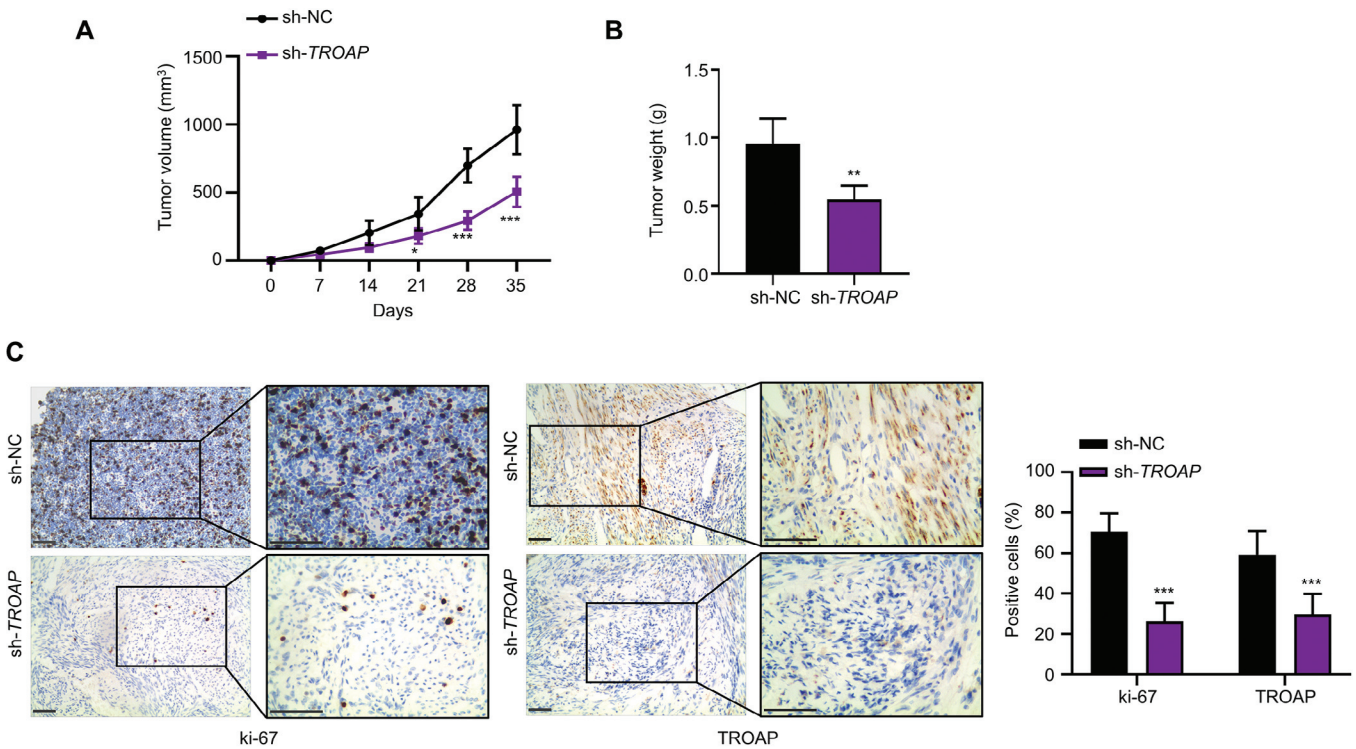

Fig. 5. Knockdown of *TROAP* inhibits tumorigenesis of EC cells *in vivo*. **A.** Tumor volume measurements of subcutaneous xenografts derived from HEC1A cells (sh-NC vs. sh-TROAP). *TROAP* knockdown significantly reduced tumor growth. **B.** Final tumor weights of HEC1A xenografts (sh-NC vs. sh-TROAP). *TROAP* knockdown resulted in significantly lower tumor weights. **C.** Immunohistochemical staining for Ki-67 and TROAP in xenograft tumor sections. *TROAP*-knockdown tumors showed reduced expression of both Ki-67 and TROAP. Scale bars, 50 μm. *p<0.05, **p<0.01, ***p<0.001 compared with the sh-NC group.

gynecological malignancy (Watanabe et al.,2021). Despite extensive research, treatment options for advanced and recurrent EC remain limited, with no significant improvement in overall survival (Callender et al., 2019). The high mortality rate of EC is largely attributed to tumor invasion and metastasis (Gonzalez-Orozco et al., 2021). Glycolysis plays a crucial role in tumor progression and serves as a critical marker of solid tumor growth, infiltration, and metastasis (Martinez-Reyes and Chandel, 2021). Targeting glycolysis regulation has emerged as a potential therapeutic strategy for EC (Chelakkot et al., 2023). Therefore, identifying molecular targets that can simultaneously inhibit tumor cell migration and invasion and regulate glycolysis is crucial for developing effective EC treatments. Our study revealed consistent *TROAP* overexpression in EC. Functional experiments demonstrated that high levels of TROAP protein expression are required for the malignant features of EC cells, and its expression negatively correlates with EC patient prognosis. These findings suggest that *TROAP* plays a significant role in EC initiation and progression.

In solid tumors, rapid growth and inadequate vascularization lead to oxygen deficiency. This forces tumor cells to rely on anaerobic fermentation for energy, resulting in lactic acid accumulation. Intracellular acidification can inhibit cell growth (Martinez-Outschoorn et al., 2017), while extracellular lactic acid creates an acidic tumor microenvironment. This acidic environment promotes tumor proliferation, invasion, and metastasis, while also fostering an immunosuppressive milieu (Cascone et al., 2018; Wang et al., 2021). Our study revealed significantly reduced lactic acid levels in the supernatant of *TROAP*-knockdown EC cells. This suggests that TROAP facilitates lactic acid export from EC cells, contributing to the formation of an acidic microenvironment. Consequently, TROAP may promote EC cell proliferation and metastasis through this mechanism.

E2F1 is a transcriptional regulator belonging to the E2F transcription factor family (Iglesias et al., 2020). Abnormal E2F1 expression in various tumors is associated with grading, staging, proliferation, and metastasis (He et al., 2018). E2F1 regulates glucose uptake in small-cell lung cancer cells and lactate production in the tumor microenvironment (Zhao et al., 2019). As a key cell cycle regulator, E2F1 activates genes facilitating G1 to S phase transition and chromosomal DNA replication (Degregori, 2002). Its overexpression promotes oncogenic transformation in various tumors by stimulating pluripotent stromal cells (Degregori, 2002) and controls EC cell proliferation (Wang et al., 2023). Our study revealed *E2F1* overexpression in EC, which significantly enhanced the proliferation, metastasis, and glycolysis of EC cells. As a transcription factor, E2F1 regulates downstream genes by binding to their promoter regions. We observed a strong correlation between *E2F1* and *TROAP* expression. Analysis of the *TROAP* promoter revealed multiple E2F1 binding sites. A dual luciferase reporter assay confirmed the ability of E2F1 to regulate *TROAP* expression. These findings suggest that E2F1 transcriptionally activates *TROAP*, potentially driving its overexpression in EC.

This study has several limitations that should be addressed in future research. Firstly, while we demonstrated the oncogenic role of TROAP in EC, our sample size was relatively small, and a larger cohort would be beneficial to validate these findings. Secondly, our study focused primarily on *in vitro* and xenograft models, which may not fully recapitulate the complex tumor microenvironment of EC. A significant limitation is the lack of investigation into how E2F1 becomes activated in EC, which could provide valuable insights into the upstream regulation of this pathway. Furthermore, while we observed the effects of TROAP on EC cell behaviors, we did not fully elucidate the molecular mechanisms by which TROAP regulates these cellular processes. Understanding these mechanisms could reveal potential therapeutic targets and provide a more comprehensive picture of the role of *TROAP* in EC progression.

In conclusion, our study reveals that transcription factor E2F1 positively regulates *TROAP* expression in EC. Overexpression of *TROAP* may function to promote cell proliferation, mobility, and glycolysis, potentially contributing to EC progression. These findings highlight the E2F1-*TROAP* axis as a potential therapeutic target and prognostic biomarker of EC. Future research should focus on elucidating the detailed molecular mechanisms of the action of *TROAP* in EC and exploring its potential as a therapeutic target.

Acknowledgements. Not applicable.

Ethics approval. The study procedures complied with the ethical standards set by the Ethics Committee of Yantai Yuhuangding Hospital (2018102603, approved on Oct 26, 2018). Informed consent for clinical research was obtained from the patients.

Each animal experimental procedure gained approval from the Animal Ethics Committee of Yantai Yuhuangding Hospital (20230094, approved on Mar 23, 2023). The experimental protocol was performed in accordance with the relevant guidelines and regulations of the Basel Declaration.

Consent for publication. All authors approved the final version and agreed with the publication.

Availability of data and materials. The datasets used and/or analyzed during the current study are available from the corresponding author via email request.

Competing interests. The authors declare that they have no conflict of interest.

Funding. None.

Authors' contributions. Conception and design: Beibei Xin, Shanshan Wang, Ping Zhu. Data analysis and interpretation: Shanshan Wang, Yidan Sun. Manuscript writing: All authors. Manuscript revision: Shanshan Wang, Minjing Guo, Ping Zhu. Final approval of manuscript: All authors.

References

Brooks R.A., Fleming G.F., Lastra R.R., Lee N.K., Moroney J.W., Son C.H., Tatebe K. and Veneris J.L. (2019). Current recommendations and recent progress in endometrial cancer. CA Cancer J. Clin. 69, 258-279.

Callender V.D., Alexis A.F., Stein Gold L.F., Lebwohl M.G., Paller A.S., Desai S.R., Tan H., Ports W.C., Zielinski M.A. and Tallman A.M. (2019). Efficacy and safety of crisaborole ointment, 2%, for the treatment of mild-to-moderate atopic dermatitis across racial and ethnic groups. Am. J. Clin. Dermatol. 20, 711-723

Cascone T., Mckenzie J.A., Mbofung R.M., Punt S., Wang Z., Xu C., Williams L.J., Wang Z., Bristow C.A., Carugo A., Peoples M.D., Li L., Karpinets T., Huang L., Malu S., Creasy C., Leahey S.E., Chen J., Chen Y., Pelicano H., Bernatchez C., Gopal Y. N. V., Heffernan T. P., Hu J., Wang J., Amaria R.N., Garraway L.A., Huang P., Yang P., Wistuba, Ii, Woodman S.E., Roszik J., Davis R.E., Davies M. A., Heymach J.V., Hwu P. and Peng W. (2018). Increased tumor glycolysis characterizes immune resistance to adoptive T cell therapy. Cell. Metab. 27, 977-987.e4.

Chelakkot C., Chelakkot V.S., Shin Y. and Song K. (2023). Modulating glycolysis to improve cancer therapy. Int. J. Mol. Sci. 24, 2606.

Degregori J. (2002). The genetics of the E2F family of transcription factors: shared functions and unique roles. Biochim. Biophys. Acta 1602, 131-150.

Fukuda M.N. and Sugihara K. (2012a). Cell adhesion molecules in human embryo implantation. Sheng Li Xue Bao 64, 247-258.

Fukuda M.N. and Sugihara K. (2012b). Trophinin in cell adhesion and signal transduction. Front. Biosci. (Elite Ed). 4, 342-350.

Fukuda M.N., Sato T., Nakayama J., Klier G., Mikami M., Aoki D. and Nozawa S. (1995). Trophinin and tastin, a novel cell adhesion molecule complex with potential involvement in embryo implantation. Genes Dev. 9, 1199-1210.

Gonzalez-Orozco J.C., Gaona-Dominguez S. and Camacho-Arroyo I. (2021). *In Vitro* models for studying tumor progression. Methods Mol. Biol. 2174, 193-206.

He J., Zhao Y., Zhao E., Wang X., Dong Z., Chen Y., Yang L. and Cui H. (2018). Cancer-testis specific gene OIP5: a downstream gene of E2F1 that promotes tumorigenesis and metastasis in glioblastoma by stabilizing E2F1 signaling. Neuro Oncol. 20, 1173-1184.

Iglesias P., Seoane M., Golan I., Castro-Piedras I., Fraga M., Arce V. M. and Costoya J. A. (2020). PARP1 deficiency reduces tumour growth by decreasing E2F1 hyperactivation: A novel mechanism in the treatment of cancer. Cancers 12, 2907.

Jiao Y., Li Y., Lu Z. and Liu Y. (2019). High trophinin-associated protein expression is an independent predictor of poor survival in liver cancer. Dig. Dis. Sci. 64, 137-143.

Li K., Zhang R., Wei M., Zhao L., Wang Y., Feng X., Yang Y., Yang S. and Zhang L. (2019). TROAP promotes breast cancer proliferation and metastasis. Biomed. Res. Int. 2019, 6140951.

Lian Y., Fan W., Huang Y., Wang H., Wang J., Zhou L., Wu X., Deng M. and Huang Y. (2018). Downregulated trophinin-associated protein plays a critical role in human hepatocellular carcinoma through upregulation of tumor cell growth and migration. Oncol. Res. 26, 691-701.

Martinez-Outschoorn U.E., Peiris-Pages M., Pestell R.G., Sotgia F. and Lisanti M. P. (2017). Cancer metabolism: a therapeutic perspective. Nat. Rev. Clin. Oncol. 14, 11-31.

Martinez-Reyes I. and Chandel N.S. (2021). Cancer metabolism: Looking forward. Nat. Rev. Cancer 21, 669-680.

Retis-Resendiz A.M., Gonzalez-Garcia I.N., Leon-Juarez M., Camacho-Arroyo I., Cerbon M.and Vazquez-Martinez E.R. (2021). The role of epigenetic mechanisms in the regulation of gene expression in the cyclical endometrium. Clin. Epigenetics 13, 116.

Siegel R.L., Miller K. D., Fuchs H. E. and Jemal A. (2022). Cancer statistics, 2022. CA Cancer J. Clin. 72, 7-33.

Urick M. E. and Bell D. W. (2019). Clinical actionability of molecular targets in endometrial cancer. Nat. Rev. Cancer 19, 510-521.

Walsh C.S., Hacker K.E., Secord A.A., Delair D.F., Mccourt C. and Urban R. (2023). Molecular testing for endometrial cancer: An SGO clinical practice statement. Gynecol. Oncol. 168, 48-55.

Wang Z.H., Peng W.B., Zhang P., Yang X. P. and Zhou Q. (2021). Lactate in the tumour microenvironment: From immune modulation to therapy. EBioMedicine 73, 103627.

Wang R., Zhang C., Guan W. and Yang Q. (2023). miRNA-329-3p suppresses proliferation and metastasis of endometrial carcinoma through downregulating E2F1. Neoplasma 70, 566-579.

Watanabe T., Nanamiya H., Kojima M., Nomura S., Furukawa S., Soeda S., Tanaka D., Isogai T., Imai J.I., Watanabe S. and Fujimori K. (2021). Clinical relevance of oncogenic driver mutations identified in endometrial carcinoma. Transl. Oncol. 14, 101010.

Xu T., Ding H., Chen J., Lei J., Zhao M., Ji B., Chen Y., Qin S. and Gao Q. (2022). Research progress of DNA methylation in endometrial cancer. Biomolecules 12, 938.

Zhao M., Liu Y., Chang J., Qi J., Liu R., Hou Y., Wang Y., Zhang X., Qiao L. and Ren L. (2019). ILF2 cooperates with E2F1 to maintain mitochondrial homeostasis and promote small cell lung cancer progression. Cancer Biol. Med. 16, 771-783.

Zhao Z.Q., Wu X.J., Cheng Y.H., Zhou Y.F., Ma X.M., Zhang J., Heng X.Y. and Feng F. (2021). TROAP regulates cell cycle and promotes tumor progression through Wnt/β-Catenin signaling pathway in glioma cells. CNS Neurosci. Ther. 27, 1064-1076.

Accepted October 16, 2024